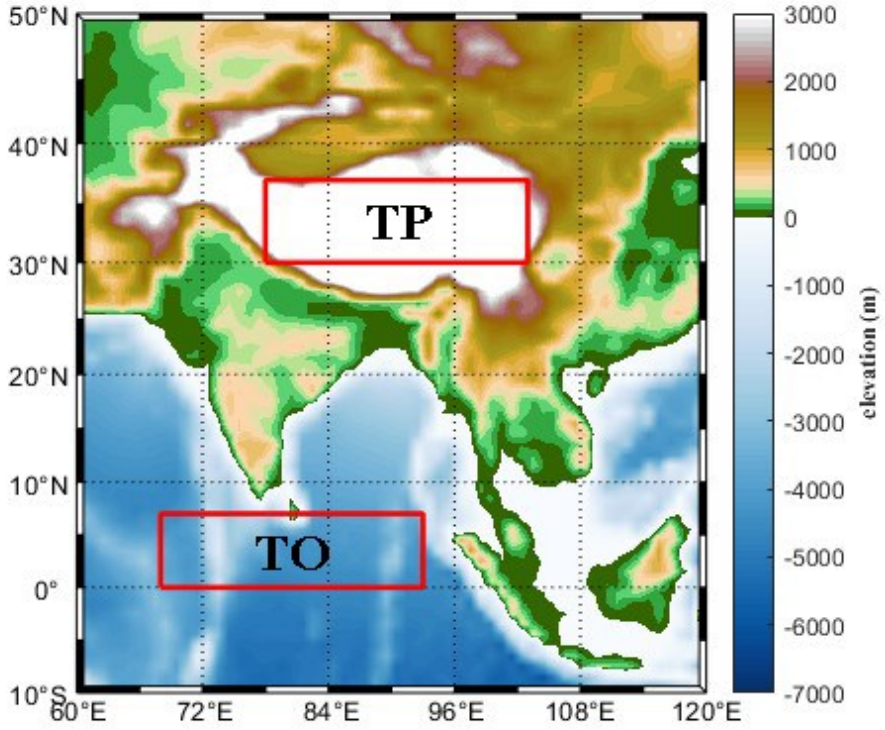

Fig. S1. The geographical location of the TP (30°N–37°N, 78°E–103°E), and TO (0°–7°N, 68°E–93°E) regions for this study.

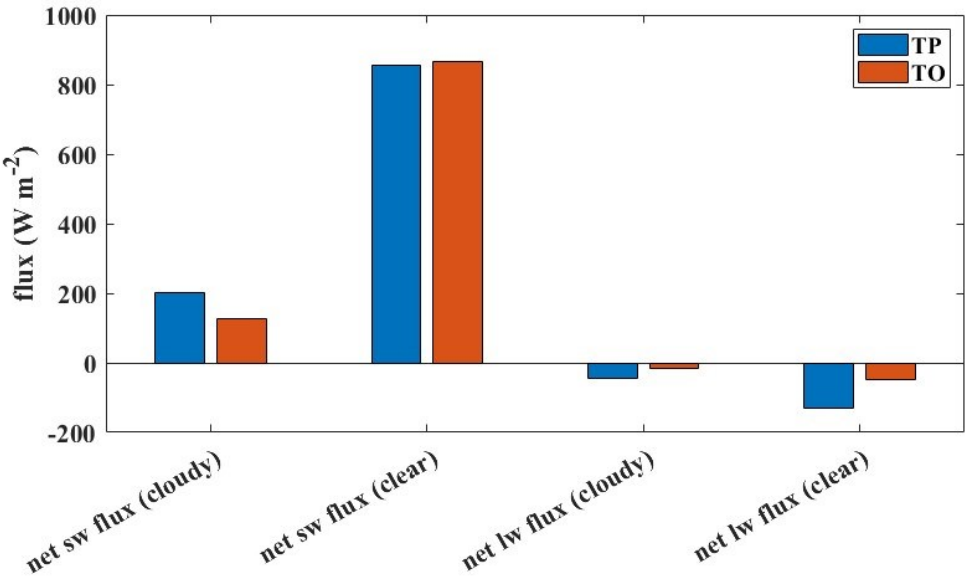

Fig. S2. The net SW flux (W m^{-2}) and LW flux (W m^{-2}) under cloudy (all-sky) or clear-sky conditions of DCCs in different regions at BOA.

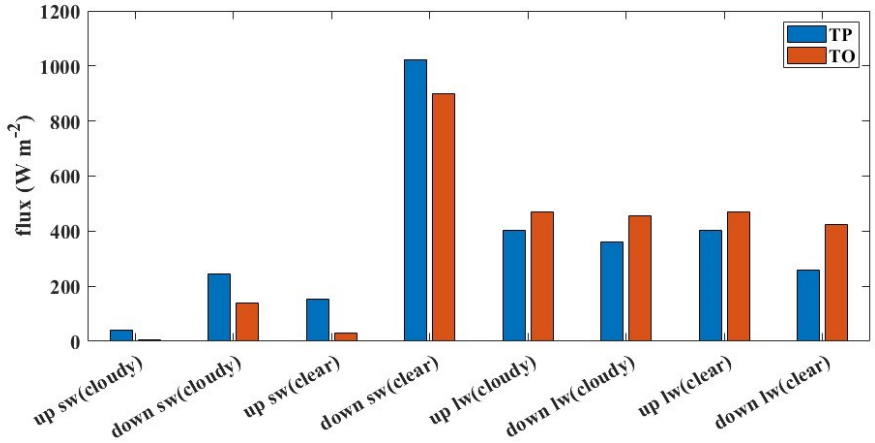

Fig. S3. The upwelling and downwelling SW flux (W m^{-2}) and LW flux (W m^{-2}) under cloudy (all-sky) or clear-sky conditions of DCCs in different regions at BOA.

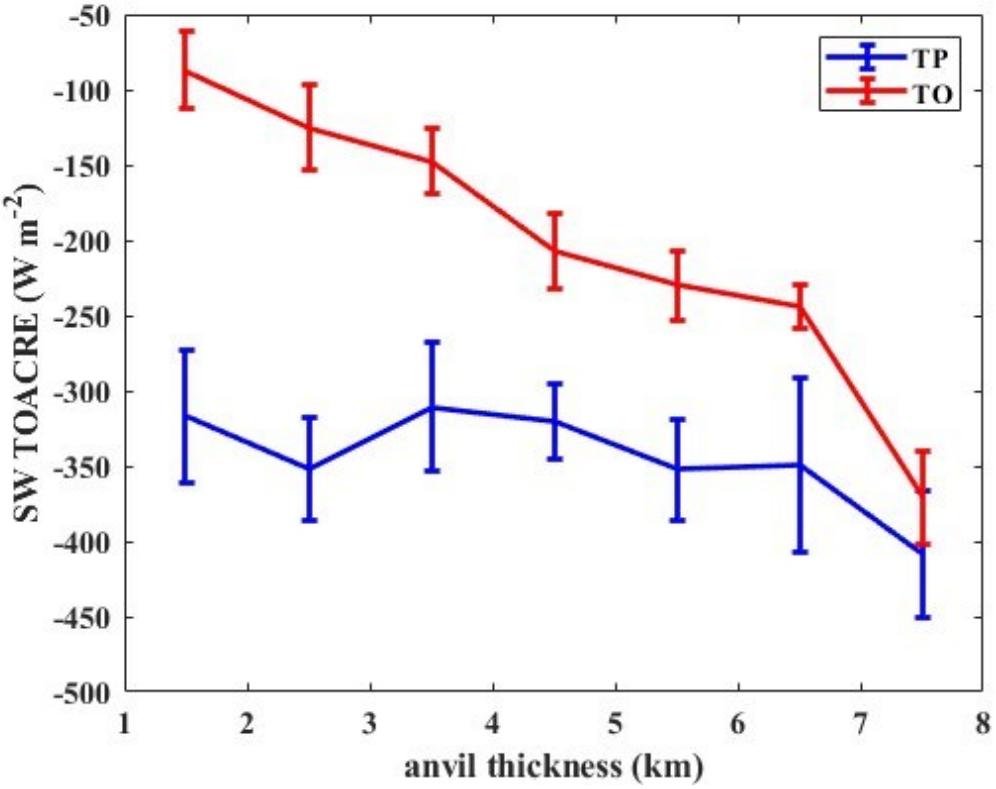

Fig. S4. Bin-averaged SW TOA CRE (W m^{-2}) of anvil and the thickness of anvil (km) in the TO. The error bars represent the standard error of the mean (SEM=standard error / √n).

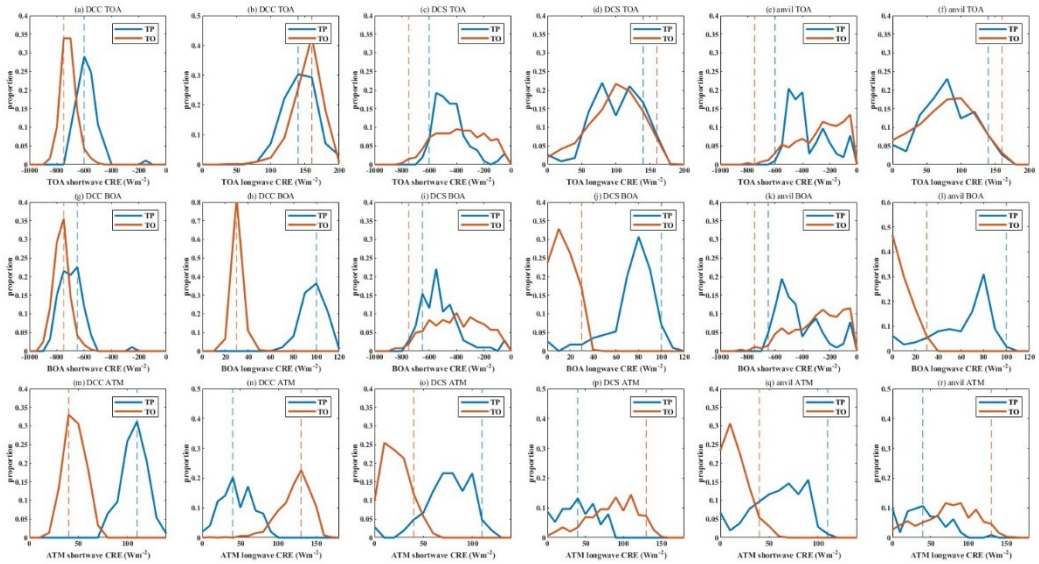

Fig. S5. The proportion of each bin of the LW CRE, the SW CRE at TOA, BOA, and ATM in the total sample of the TP (blue), and TO (red). The dash lines show the peak of DCC.

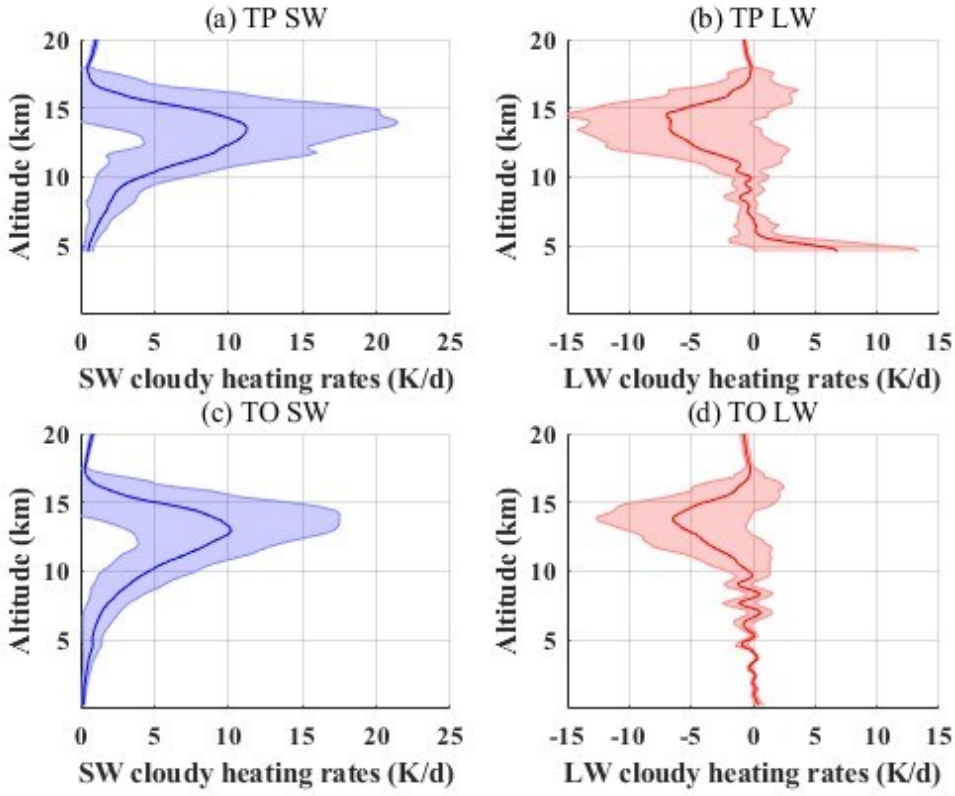

Fig. S6. The mean vertical profiles of cloudy (all-sky) heating rates (K/d) of DCCs over the TP, and TO. The shadow range represents the standard deviation.

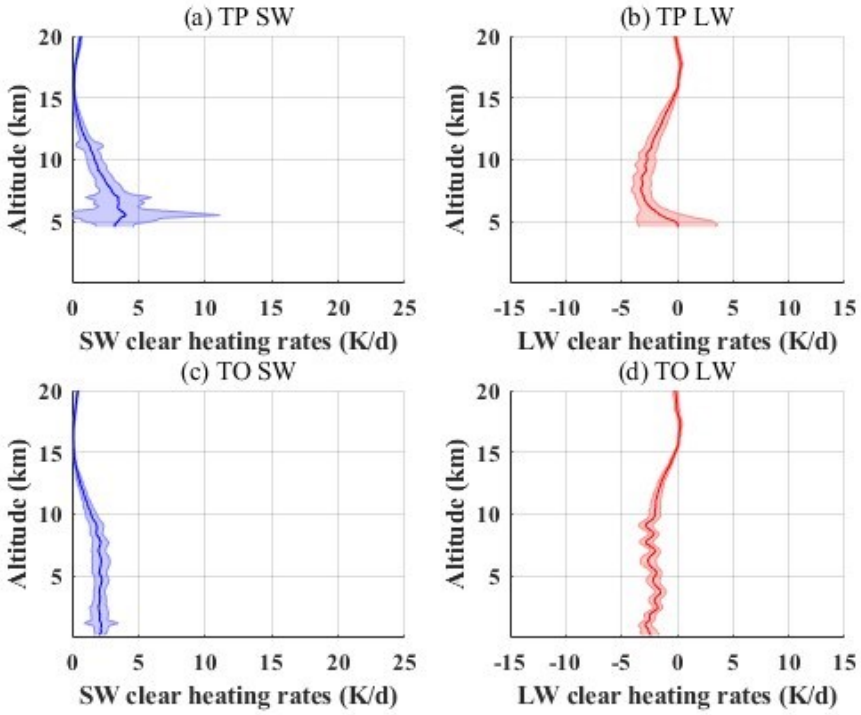

Fig. S7. The mean vertical profiles of clear-sky heating rates (K/d) of DCCs over the TP, and TO. The shadow range represents the standard deviation.

Region	TOA CRE (W m^{-2})					
	SWCRE			LWCRE		
	DCC	DCS	anvil	DCC	DCS	anvil
TP	-559.5	-418.0	-338.4	152.3	110.7	89.4
TO	-688.8	-348.8	-246.2	162.4	108.1	88.8
Region	BOA CRE (W m^{-2})					
	SWCRE			LWCRE		
	DCC	DCS	anvil	DCC	DCS	anvil
TP	-671.9	-498.0	-401.3	102.2	78.7	65.8
TO	-739.4	-375.4	-266.2	35.5	18.7	13.1

Table S1. The SW CRE (W m-2) and LW CRE (W m-2) at TOA and BOA of DCSs, DCCs and anvil in different regions.

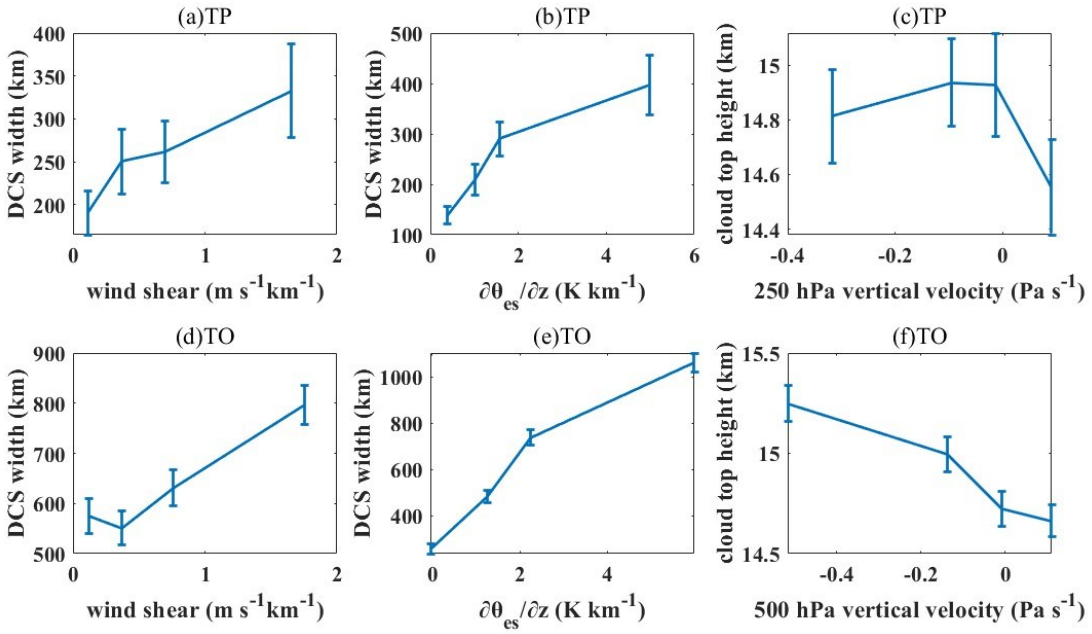

Fig. S8. Bin-averaged wind shear (m $s^{-1}km^{-1}$; a, d), the vertical gradient of the saturated equivalent potential temperature $\partial\theta_{es}/\partial z$ (K km^{-1}; b, e) and vertical velocity (Pa s^{-1}; c, f) with DCSs width (km) and cloud top height (km) from different regions. The error bars represent the standard error of the mean (SEM=standard error / $\sqrt{n}$).

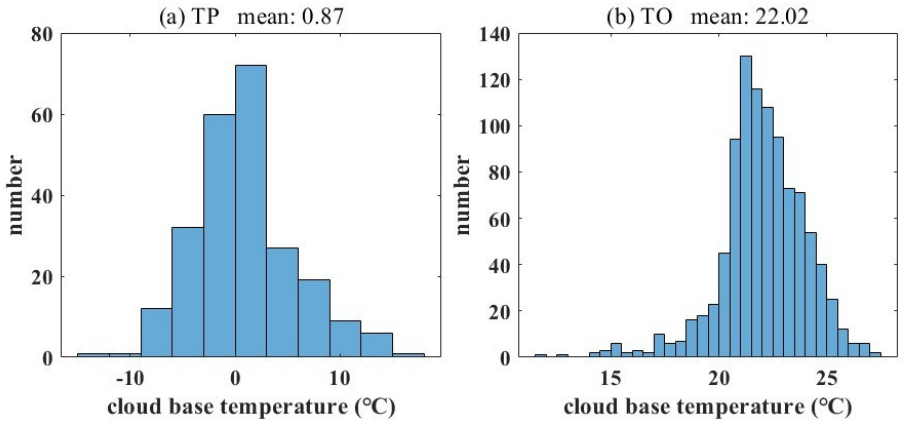

Fig. S9. Histogram of cloud base temperature (℃) of DCCs in the TP (a), and TO (b). And the mean cloud base temperature (℃) of DCCs in different regions.

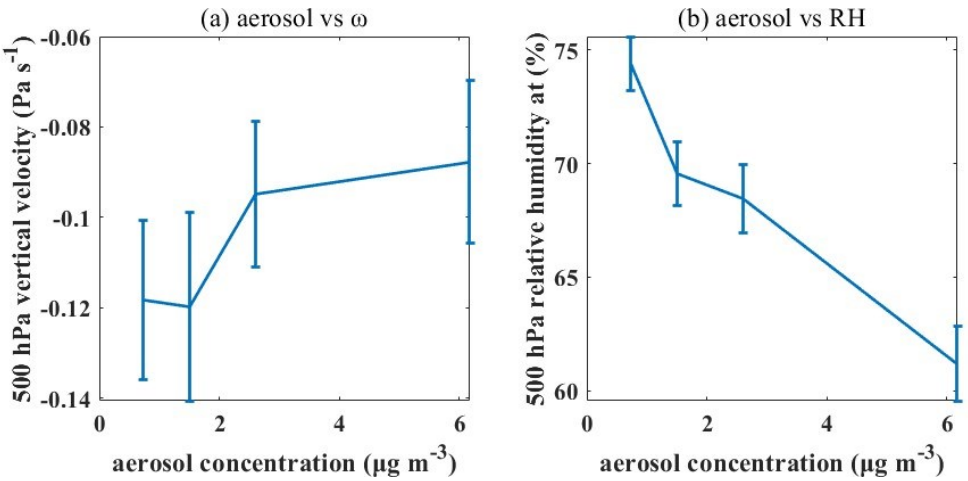

Fig. S10. Bin-averaged 500 hPa vertical velocity (Pa s^{-1}; a) and 500 hPa relative humidity (%; b) with aerosol concentration (μg m^{-3}) of DCCs in the TO. The error bars represent the standard error of the mean (SEM=standard error / $\sqrt{n}$).